Title: Materials Characterization of Impregnated W and W-Ir Cathodes after Oxygen Poisoning

Author: James E. Polk Angela M. Capece

PII: S0169-4332(15)00432-8
DOI: http://dx.doi.org/doi:10.1016/j.apsusc.2015.02.116
Reference: APSUSC 29796

To appear in: *APSUSC*

Received date: 10-11-2014
Revised date: 15-2-2015
Accepted date: 16-2-2015

Please cite this article as: James E. Polk, Angela M. Capece, Materials Characterization of Impregnated W and W-Ir Cathodes after Oxygen Poisoning, *Applied Surface Science* (2015), http://dx.doi.org/10.1016/j.apsusc.2015.02.116

Highlights:

- Hollow cathodes with impregnated tungsten and tungsten-iridium emitters were operated with 100 ppm of oxygen in the xenon gas flow for 480 and 80 hours, respectively.
- Chemical and morphological changes were studied using scanning electron microscopy, energy dispersive spectroscopy, and laser profilometry.
- High concentrations of oxygen accelerate the formation of tungstate layers in both types of emitters.
- Deposits of pure tungsten were observed on the W-Ir emitter, indicating that tungsten is preferentially removed from the and transported in the insert plasma.
- The W-Ir emitter exhibited less erosion and redeposition at the upstream end than the pure W emitter surface.

Materials Characterization of Impregnated W and W-Ir Cathodes after Oxygen Poisoning

James E. Polk[a,*], Angela M. Capece[1]

California Institute of Technology, 1200 E. California Blvd., Pasadena, CA 91125

[a] *Jet Propulsion Laboratory, California Institute of Technology, 4800 Oak Grove Dr., Pasadena, CA 91109*

Abstract

Electric thrusters use hollow cathodes as the electron source for generating the plasma discharge and for beam neutralization. These cathodes contain porous tungsten emitters impregnated with BaO material to achieve a lower surface work function and are operated with xenon propellant. Oxygen contaminants in the xenon plasma can poison the emitter surface, resulting in a higher work function and increased operating temperature. This could lead directly to cathode failure by preventing discharge ignition or could accelerate evaporation of the BaO material. Exposures over hundreds of hours to very high levels of oxygen can result in increased temperatures, oxidation of the tungsten substrate, and the formation of surface layers of barium tungstates. In this work, we present results of a cathode test in which impregnated tungsten and tungsten-iridium emitters were operated with 100 ppm of oxygen in the xenon plasma for several hundred hours. The chemical and morphological changes were studied using scanning electron microscopy, energy dispersive spectroscopy, and laser profilometry. The results provide strong evidence that high concentrations of oxygen accelerate the formation of tungstate layers in both types of emitters, a phenomenon not inherent to normal cathode operation. Deposits of pure tungsten were observed on the W-Ir emitter, indicating that tungsten is preferentially removed from the surface and transported in the insert plasma. A W-Ir cathode surface will therefore evolve to a pure W composition, eliminating the work function benefit of W-Ir. However, the W-Ir emitter exhibited less erosion and redeposition at the upstream end than the pure W emitter.

Keywords: cathodes, oxygen poisoning, barium tungstate

1. Introduction

Hollow cathode electron sources are one of the key life-limiting components in electric thrusters. These thrusters are required to operate for tens of thousands of hours, which places extraordinary demands on component reliability. State-of-the-art hollow cathodes consist of a refractory metal cathode tube that houses a porous tungsten emitter (also called the "insert"). Xenon propellant is injected through the hollow cathode, and an orifice plate downstream serves to increase the internal pressure in the insert region. A heater surrounding the cathode is used to heat the cathode until it reaches the temperature required to ignite a discharge which generates an internal xenon plasma. This plasma helps conduct the current into the main discharge and heats the insert, so the discharge becomes self-sustaining.

A low emitter operating temperature is achieved by maintaining a layer of adsorbed oxygen and barium atoms on the tungsten substrate, which lowers the surface work function[1]. Ba and BaO are supplied by BaO-CaO-Al_2O_3 source material that is impregnated in the pores of the tungsten. Gaseous Ba and BaO are released in interfacial reactions between the tungsten matrix and the impregnant. The Ba and BaO then migrate to the surface by Knudsen flow and surface diffusion on the pore walls, replenishing Ba and O adsorbates lost by evaporation.

Cathodes for electric thrusters are typically operated in current-controlled mode, and therefore, degradation of the surface emission properties results in an increase in the operating temperature in order to sustain the required current density. The emission properties of the surface can change when the tungsten pores are blocked and Ba cannot migrate to the surface, the Ba supply in the interior is depleted, or chemical changes occur at the surface that modify the work function.

Reactive gases, which may be introduced into the xenon flow via leaks, propellant impurities, and residual chemicals in the feed system, have been shown to cause a significant increase in the work function of impregnated cathodes in vacuum devices [2, 3]. This poisoning can lead directly to cathode failure by preventing discharge ignition, or accelerate other failure mechanisms. For example, a higher operating temperature due to increased work function ac-

*Corresponding author

Email address: james.e.polk@jpl.nasa.gov (James E. Polk)

[1] Current address: Princeton Plasma Physics Laboratory, Princeton, New Jersey 08543, USA.

celerates the evaporation of Ba from the surface and the reaction between the impregnant and the tungsten, leading to more rapid depletion of the barium supply. The formation of solid barium tungstate layers has been observed on portions of the cathode emitter surface in several long duration tests [4, 5, 6]. $BaWO_4$ is a poor electron emitter and a stable product of the reaction between the impregnant and the tungsten matrix[7], so it will not act as an electron source or provide Ba or BaO to replenish the adsorbates on the tungsten surfaces in the insert. In addition, the thick solid layers close off the pores in the tungsten and likely prevent the release of Ba from below. These products were initially observed in tests with leaky gas systems[4], and were not found on inserts from two long duration tests with carefully controlled gas feed systems[8, 9]. Therefore, it appears that excess oxygen may accelerate the formation of these layers. Basic thermochemistry calculations support this conclusion[11].

Additionally, tungsten deposition on the orifice plate and emitter surface has been observed in many extended hollow cathode tests[4, 5, 8, 9]. Cathode operating temperatures are not high enough to cause significant evaporation of the tungsten matrix, so this is likely due to the formation and subsequent dissociation of volatile tungsten compounds. Detailed examination of cathodes from two long duration tests[8, 9] shows that there is net erosion in the emission zone, but redeposition of tungsten forms a less porous shell on the surface that restricts the flow of Ba and BaO and suppresses impregnant reactions. Modeling showed that the Ba that replenishes the emission zone is released upstream and transported through the gas phase[10]. No failures have been attributed to these material transport processes, but they could potentially lead to cathode failure. Reduction in the cathode orifice diameter by deposition of tungsten eroded from internal surfaces could increase the operating temperature or prevent cathode ignition, and deposits of tungsten on the emitter surface may eventually limit the amount of Ba that can be released from the tungsten matrix.

The lack of understanding of the chemical and mass transport processes in hollow cathodes has prevented development of useful models for these failure processes. Laboratory and flight systems now employ costly and time-consuming propellant system purification and handling procedures that guarantee the minimum detectable level of reactive contaminants, because it is unclear if higher levels are tolerable.

The focus of this paper is on an experiment designed to study the chemical and morphological changes on impregnated hollow cathodes resulting from long duration exposure to oxygen. Tungsten and tungsten-iridium inserts were operated with 100 ppm of oxygen in the xenon plasma discharge for 480 and 80 hours, respectively, and then underwent destructive analyses to study changes in the surface morphology and chemical state using SEM, EDS, and laser profilometry.

W-Ir cathodes are under investigation as a potential replacement for conventional W inserts because they offer a number of potential lifetime benefits due to a lower work function and lower evaporation rates of Ba from the surface[13]. W-Ir is also expected to be less reactive with oxygen and water vapor, although there is little quantitative data on this potential benefit. The work presented here is part of an effort to gain insights into the physical processes occurring on the insert surface for more accurate cathode life assessments and to help define better guidelines for propellant and feed system cleanliness.

2. Experimental Setup

The cathode experiments, which are described in further detail in Ref. [14, 15], were conducted in a vacuum facility at a base pressure of 10^{-6} Torr. The cathode is of the standard configuration shown in the drawing in Fig. 1. The cathode tube, which houses the insert, is made of molybdenum-rhenium and incorporates a tungsten orifice plate with a 1 mm diameter orifice. The experiments were conducted with a conventional porous tungsten insert and a mixed metal matrix insert made with an 80:20 wt% tungsten-iridium alloy, both impregnated with a 4:1:1 molar ratio of BaO-CaO-Al_2O_3.

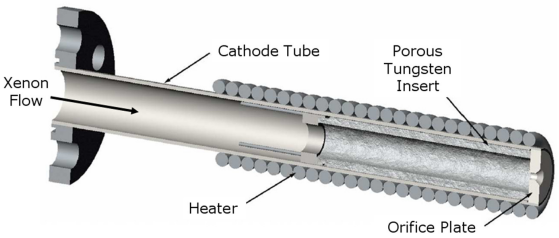

Figure 1: Sectioned view of the cathode.

Propellant-grade xenon (99.9995% purity) was injected through the hollow cathode. Research grade oxygen (99.999% purity) was used as the poisoning gas. The oxygen feed system was designed to produce oxygen concentrations in the xenon flow ranging from 0.1 to over 100 parts per million using a fused silica capillary tube with a 20 μm inner diameter and a length of 9 m that acts as a flow restrictor. The W and W-Ir inserts were operated with 100 ppm of oxygen in the xenon discharge for durations of 480 hours and 195 hours, respectively. Following these exposures, both inserts were removed from the cathodes and cracked into several pieces to expose the interior emitting surfaces. Scanning electron microscopy (SEM) was used to characterize changes in the surface microstructure and chemistry. Photomicrographs of the new tungsten insert were obtained prior to these tests for comparison with the post-test images. The W-Ir insert was not documented before these tests; however, a new W-Ir insert from the same batch was used for comparison. Energy dispersive spectroscopy (EDS) was used to determine

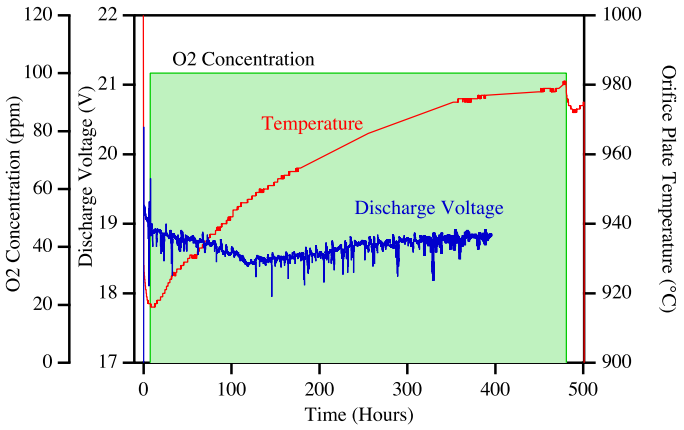

Figure 2: Effect of long term oxygen exposure on discharge voltage and temperature for the tungsten insert.

the elemental composition of the surface features, and the profiles of the interior surfaces were measured using a laser profilometer system with a resolution of less than 1 μm.

3. Tungsten Insert

The tungsten insert was operated at a discharge current of 12.85 A and a xenon flow rate of 3.35 sccm with 100 ppm of oxygen for 480 h. These values correspond to operating conditions of the NASA Solar Electric Propulsion Technology Application Readiness (NSTAR) ion thruster cathode for comparison purposes[14]. A previous short-duration exposure (1 hour) at these conditions had indicated no signs of poisoning. However, over the course of the longer exposure, the insert temperature increased monotonically by 65°C, as shown in Fig. (2). After the oxygen flow was turned off, the temperature dropped by 10°C over 7.5 h, then remained stable for the next 13 hours of operation until the cathode was turned off. The elevated temperature after cessation of the oxygen flow indicates irreversible degradation of the cathode and perhaps significant chemical and morphological changes to the emitter surface. The post-test analyses of the tungsten insert involved laser profilometry of the inner surface of the insert cylinder, SEM imaging of the surface at various axial locations, and EDS to determine the chemical composition.

The thickness and composition of the layers are summarized in Fig. (3). The solid black line is the profile of the inner surface of the insert cylinder measured post-test with laser profilometry. The original insert surface, shown as a dashed black line, was inferred from the post-test profile and the thickness of surface deposits measured in SEM images. The solid red line represents the profile measured on an insert that had never been operated. The surface profile of the unused insert (red line) was flat to within ± 5 μm except near the upstream end ($x = 25$ mm) where the indicated height drops slightly, which represents an increase in the insert inner radius of about 15 μm. This dip is

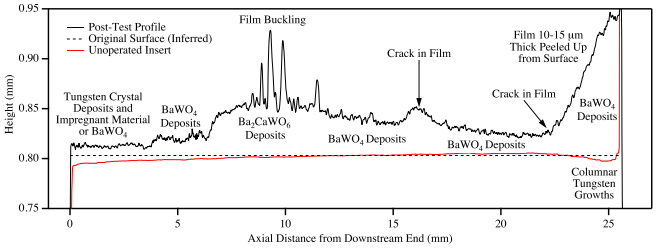

Figure 3: Measured axial profile of the inner surface of the tungsten insert cylinder after the oxygen exposure compared with the pre-test profile. The downstream end is at $x = 0$ mm, and the upstream end is at $x = 25$ mm.

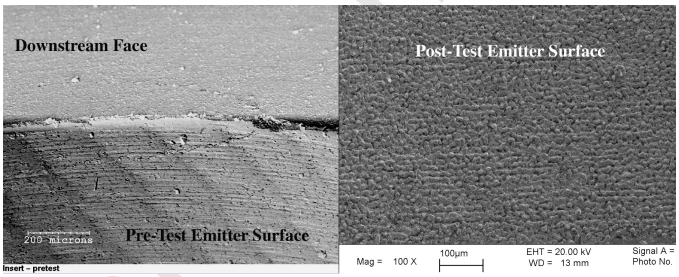

Figure 4: Comparison of insert emitter surface at high magnification before (left) and after the 480 hour oxygen exposure (right).

near the interface between the porous tungsten insert and a molybdenum ring that is brazed on the upstream end (a feature which the inserts used in the poisoning experiments do not have), and may be an artifact of machining. The inferred pre-test profile is very similar to the profile of the unoperated insert, indicating that it was machined with a similar wall thickness and tolerance.

Figure (4) shows images comparing the downstream end of the insert before and after the 480 h exposure. Machine marks are visible in the porous sintered tungsten surface prior to operation. In the images taken after the oxygen exposure, the crystal deposits appear to follow these machine marks. Fine tungsten fibers 0.5–4 μm in diameter and up to 100 μm long were found on the downstream face of the cylindrical insert, but not on the inner surface.

Figure (5) displays photomicrographs taken using backscattered electrons (BSE) at a magnification of 2000× along the length of the insert. This imaging mode produces variations in grey level that correspond to elemental differences, and in general, the lighter areas are tungsten-rich and the darker areas indicate the presence of barium. The dimension in the upper left corner of each image indicates the distance from the downstream end of the insert. The top left image in Fig. (5) shows tungsten deposits at the insert tip ($x = 0$ mm). These deposits appear to consist of isolated crystals on the original porous tungsten matrix. EDS analysis revealed that the crystals are pure tungsten, and that the darker regions contain primarily barium, oxygen, and a small amount of calcium. It is difficult to deter-

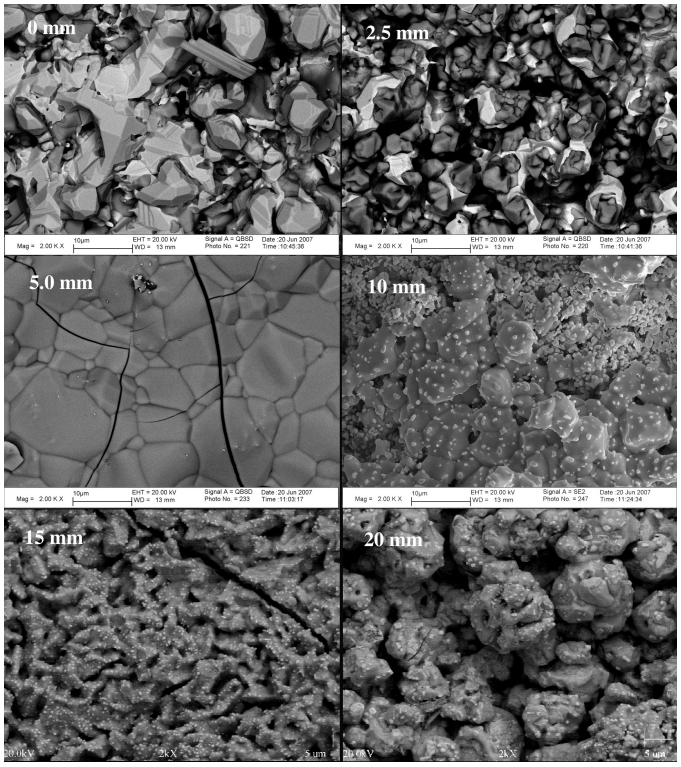

Figure 5: Photomicrographs taken with backscattered electrons at a magnification of 2000× along the length of the tungsten insert. The number in the upper left corner of each image indicates the distance from the downstream end.

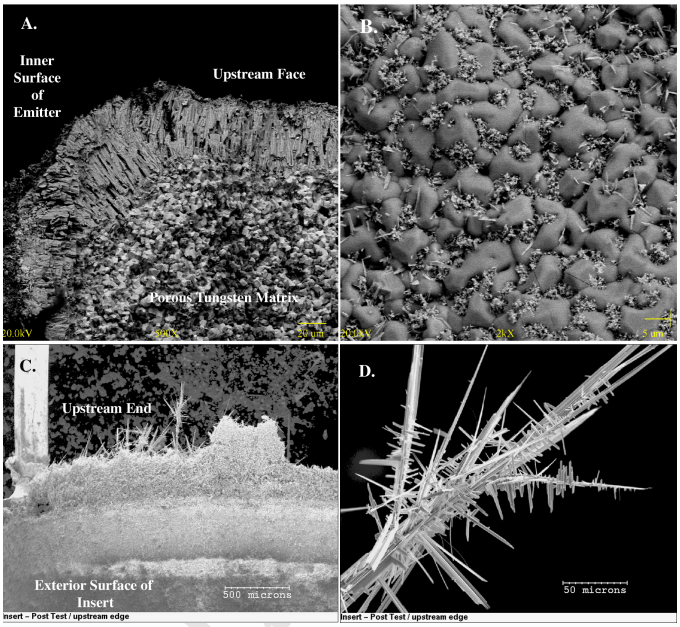

Figure 6: Photomicrographs of the upstream end of the tungsten insert. A. Fracture surface showing tungsten columnar grain growth in the inner diameter and upstream face (backscattered electron image to emphasize elemental differences. B. Tungsten whiskers growing in the low spots in a barium tungstate film on the inner surface. C. Erosion on exterior and fine tungsten whisker growth at the upstream end. D. Spectacular example of vapor-deposited tungsten crystal growth.

mine the phase of these deposits with elemental analysis alone, but they could be either unreacted impregnant material or Ba_2CaWO_6, a product of the reactions between the impregnant and tungsten [7].

The tungsten crystals have a much denser coating of the barium-containing material further upstream, as demonstrated in the top right photomicrograph of Fig. (5), taken 2.5 mm from the tip. In this location, the calcium signal is much stronger than at the tip. A very small aluminum signal was also detected. Again, this is consistent with either impregnant material, a tungstate such as Ba_2CaWO_6, or some mixture. Throughout this region, the crystals appear to be only one layer thick, contributing about 10 μm to the thickness of the insert as shown in Fig. (3).

From 3.8 mm to 6.8 mm from the tip, the deposits on the surface are about twice as thick as the deposits at $x = 2.5$ mm. SEM images revealed a dense, relatively flat coating with fine surface cracks. A backscattered electron image of this region at $x = 5$ mm is shown in the middle left image in Fig. (5). The BSE image indicates that the composition is very uniform, and EDS detected only tungsten, barium, and oxygen. These characteristics suggest that this is a coating of $BaWO_4$, which is an inert reaction product.

At 6.8 mm from the tip, the film thickness rapidly increases to 40–50 micrometers. Between $x = 9.5$ and 11.5 mm, the thick film buckled in a number of locations, leaving voids between the deposit and the underlying porous tungsten substrate. This produced the peaks in the profilometer signal in Fig. (3). The middle right image in Fig. (5) at $x = 10$ mm shows deposits consisting of lumps of tungsten, barium, calcium, and oxygen. In this case, the barium signal was comparable in intensity to the tungsten peak, suggesting that this material is Ba_2CaWO_6. The fine, light colored crystals visible in this photomicrograph are pure tungsten.

The thickness of the deposit decreases monotonically from $x = 10$ mm all the way to the upstream end of the insert at $x = 25$ mm. The deposit cracked near $x = 16$ mm and at $x = 22mm$, allowing the film to peel up from the surface, which produced features at these locations in Fig. (3). The two bottom images in Fig. (5) show some minor differences in the scale of the surface features compared with the image taken at $x = 10$ mm, although they are qualitatively similar. EDS analysis showed that the bulk deposits contained tungsten, barium, and oxygen, suggesting $BaWO_4$, while the fine crystals were pure tungsten.

An unusual feature discovered in the post-test analysis was the heavy erosion and redeposition of tungsten at the upstream end of the insert shown in Fig. (6). Fig. (6A) is a backscattered electron photomicrograph of a fracture surface which shows a cross-section of the cathode at the upstream end. The corner in this image is defined by the inner diameter of the insert and the downstream face. The

sintered metal substrate with impregnated pores is visible deep in the insert, but the outer surfaces have a deposit of columnar tungsten crystals that is up to 45 μm thick. The image in Fig. (6B) shows the tungstate deposit on the inner surface with fine tungsten whiskers growing in the depressions in the film. Fig. (6C) shows the upstream end of the insert from the exterior. An eroded region up to 0.5 mm long occurs on the outer surface at the upstream end. A dense growth of tungsten fibers covers this region. Fig. (6D) shows a detail of one of the complex tungsten fibers.

4. Tungsten-Iridium Insert

TheW-Ir cathode was exposed to 100 ppm of oxygen at a discharge current of 6 A for 47.5 hours. In a previous 3 hour exposure at these conditions, no poisoning was observed, but during the longer exposure degradation of the emitter condition became evident, as shown in Fig. (7). The temperature initially dropped by 4°C in the first 10 hours, then climbed by 15°C, while the discharge voltage increased by about 0.25 V. Both parameters returned to the initial values when the oxygen flow was stopped. A second exposure for 79.4 hours resulted in an increase in temperature of 60°C and a discharge voltage increase of 0.45 V. In this case the emitter only partially recovered when the oxygen flow was stopped. No degradation was observed at 12.35 A in a subsequent 16 hour exposure at 10 ppm, but when the oxygen concentration was increased to 100 ppm for 52.5 hours, the temperature rose by 19°CThe discharge voltage in this case was relatively constant. After the exposure, the insert recovered almost completely. The W-Ir cathode appears to be more resistant to short term poisoning compared to the tungsten cathode, but suffers similar degradation over long term exposures.

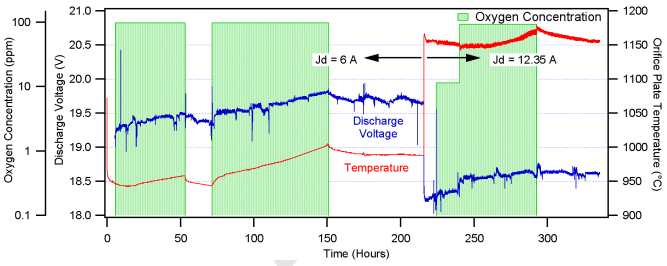

Figure 7: Effect of long term oxygen exposure on discharge voltage and temperature for the tungsten-iridium insert.

The morphology of the inner surface of the W-Ir insert is similar to that observed on the W insert, although its Ba deposits were not as thick and it did not suffer from the extreme surface modification at the upstream end. Figure (8) shows a series of photomicrographs using secondary electrons taken along the W-Ir insert length at the same magnification (2000×) as the tungsten insert images in Fig. (5). The top left and top right images in Fig. (8) show tungsten crystal deposits in the downstream emission zone at $x = 0$ mm and $x = 2.5$ mm, respectively. The crystals are 5-10 μm in diameter, and EDS indicates they are pure tungsten. These are isolated crystals on the original substrate material, in which iridium is still present. These surfaces also yield barium, calcium, oxygen, and aluminum signals, indicating the presence of impregnant material or reaction products on the surface. The barium deposits are denser at $x = 2.5$ mm than at the tip, as was observed on the tungsten insert.

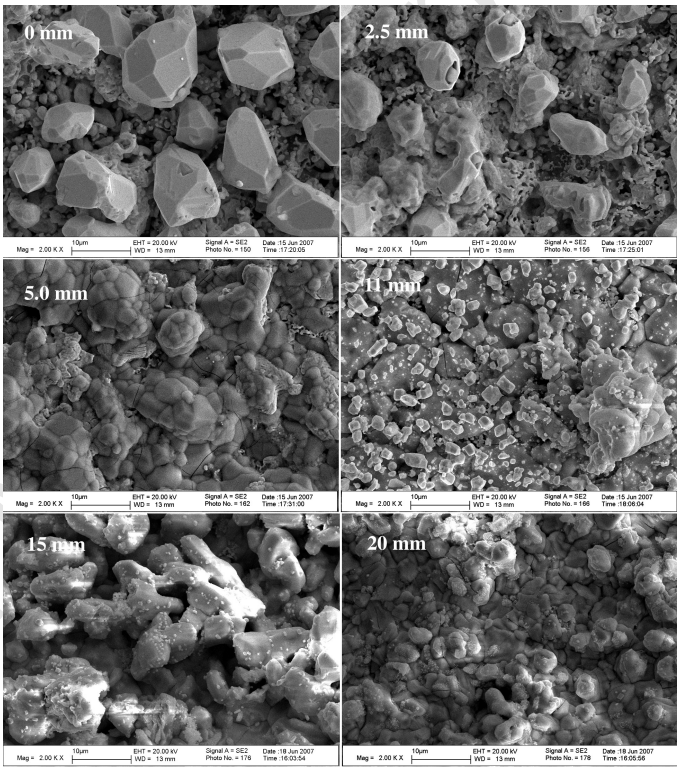

Figure 8: Photomicrographs taken with secondary electrons at a magnification of 2000× along the length of the W-Ir insert. The number in the upper left corner of each image indicates the distance from the downstream end.

The middle left image in Fig. (8) at $x = 5$ mm from the downstream end shows the surface covered with a solid coating. EDS analysis indicates that the coating contains tungsten, barium, and oxygen, but very little calcium. The morphology is similar to the $BaWO_4$ layers observed on the tungsten insert at $x = 5$ mm in Fig. (5). Further upstream at $x = 11$ mm, the tungstate layers are coated with small pure tungsten crystals, as shown in the remaining images in Fig. (8). The crystals at $x = 11$ mm, which are 1-2 μm in diameter, are somewhat larger than those found on the W insert at this same axial location. Deposits with an elemental composition of tungsten, barium, calcium, and oxygen were found on the upstream end, but no iridium was detected on the inner surface. There was no evidence of the extensive erosion and redeposition apparent on the tungsten insert.

5. Discussion

The hollow cathodes used in these experiments were operated with constant current, so an increase in work function due to poisoning results in higher operating temperatures. The long-term effects of oxygen exposure indicate that there is a mechanism for emitter degradation with a characteristic time scale of tens to hundreds of hours at 100 ppm oxygen concentration. Both cathodes experienced the growth of surface tungstate layers. Figure (9) shows the emitter temperature profile and centerline plasma density measured in tungsten inserts operated with high purity xenon expellent at 12–13 A [13, 17] overlayed on the profile of the tungsten insert shown previously in Fig. (3). The plasma density profile indicates that the discharge is confined to the first 5 mm of the insert length. The dense tungstate layers appear 3.8 mm from the downstream end and may have restricted the emission zone over time, resulting in higher temperature to support higher current density. Even at $x = 2.5$ mm, deposits of barium-containing materials covered a large fraction of the surface. If these deposits were composed of stable reaction products such as $BaWO_4$ they would have reduced the emitting area in this zone as well and would not have contributed Ba to the remaining emitting surface. It is clear from this plot that the thickest tungstate deposits occur at intermediate temperatures and relatively low plasma densities ($\leq 10^{13}$ cm^{-3}), which may be an important clue to the kinetics of tungstate surface layer formation.

As noted earlier, tungstate deposits were observed in hollow cathode tests with air leaks in the propellant feed systems [4], and the phenomena observed here are very similar. Changes in cathode behavior over a time scale of several hundred hours were also noted in these tests. Tungstate deposits were also found in the post-test examination of a hollow cathode which failed after 28,000 hours of operation at 12 A. An improved gas feed system was employed in this test, and Sarver-Verhey concluded that tungstate formation is inherent in cathode operation and is one possible failure mechanism [16]. Although $BaWO_4$ is a stable product of the reactions between the impregnant and tungsten in the pores of the insert, the formation of surface layers of $BaWO_4$ are evidently not inherent in hollow cathode operation. The insert surfaces of the discharge and neutralizer cathodes from the 8,200-hour Life Demonstration Test (LDT) and the 30,000-hour Extended Life Test (ELT) showed no signs of tungstate formation, presumable because of lower reactive contaminant levels [8, 9]. Point-of-use gas purity measurements at the beginning and end of the ELT indicated oxygen levels of 0.1 ppm or less. The results reported here provide strong evidence that high concentrations of oxygen accelerate tungstate surface layer formation in both types of inserts. These tests involved a total oxygen dose 6-16 times higher than in the ELT. At this point, it is not clear if there is a threshold oxygen level for tungstate formation. Subsequent work will focus on determining if an intermediate level of oxygen that might be achievable with less costly purification and handling procedures is tolerable.

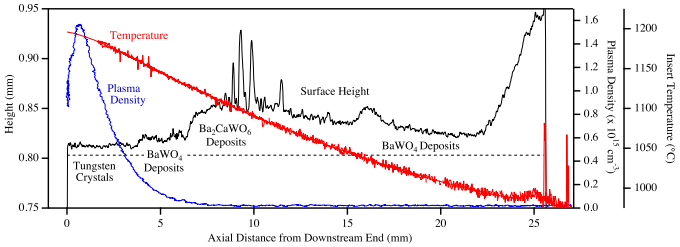

Figure 9: W insert temperature profile and centerline plasma density overlayed onto the measured axial profile of the W insert cylinder after the oxygen exposure.

Tungsten crystal deposits were found at the downstream end of both inserts, although in much lower quantities than typically found in longer duration tests with lower total oxygen doses. For example, in the ELT and the LDT, erosion and subsequent redeposition of tungsten in the emission zone had formed a dense tungsten shell on the surface [12]. The lower tungsten deposition rates found in the poisoning experiments could indicate that another species is the culprit, or that the rate of erosion or subsequent redeposition is not controlled by the oxygen partial pressure. The W-Ir cathode deposits were composed of pure tungsten, indicating that tungsten is preferentially removed from the surface and transported in the insert plasma. The 80-20 wt% W-Ir composition consists of two phases; a W-solid solution containing less than 5 at% Ir and an intermetallic with an approximate composition of 50 at% W-50 at% Ir. The solid solution phase is likely the source of the tungsten deposits, which would explain the lack of Ir in them. Because tungsten is preferentially deposited at the downstream end in the emission zone in W-Ir cathodes, the benefits of the lower work function from the intermetallic phase will eventually be lost as it is covered up.

One major difference between the two inserts was the extent of erosion and redeposition at the upstream end. This is another phenomenon found in early tests with air leaks in the gas feed systems [4] that has not been observed in recent tests with improved feed systems. The absence of this phenomenon in the W-Ir insert may be an indication of greater oxidation resistance or simply the result of lower temperature at the upstream end and less time operating at elevated oxygen levels.

6. Conclusions

These experiments have yielded several contributions to our understanding of reactive gas impurity effects on hollow cathodes. First, they revealed the effect of large oxygen exposures on cathode operation. The temperature of both the W and W-Ir inserts increased by at least 60°C, and the temperature remained high even after oxygen flow

ceased, indicating significant chemical and morphological changes to the emitter surface. Second, tungsten deposition in the emission zone was observed; this process could lead to degraded performance on an even longer time scale by reducing barium flow to the surface. Third, these results provide a strong link between elevated oxygen levels in the gas and the formation of bulk tungstate layers on the emitter surface. Contrasting these results with the lack of tungstate formation in the ELT and LDT cathodes suggests that this failure mechanism is not necessarily inherent in hollow cathode operation, but occurs in systems with elevated oxygen levels. Finally, the major difference between the two inserts was the extent of erosion and redeposition at the upstream end. The absence of this phenomenon in the W-Ir insert may be an indication of greater oxidation resistance or simply the result of lower temperature at the upstream end and less time operating at elevated oxygen levels.

7. Acknowledgements

The authors would like to thank Al Owens, Ray Swindlehurst, and Ron Watkins for their assistance in preparing the test facility and Ron Ruiz and Jim Kulleck for their contributions in electron microscopy. The research described in this paper was carried out by the Jet Propulsion Laboratory, California Institute of Technology, under a contract with the National Aeronautics and Space Administration.

References

[1] P. Palluel, A.M. Schroff, Experimental Study of Impregnated-Cathode Behavior, Emission, and Life, J. Appl. Phys. 51 (1980) 2894–2902.

[2] J. Cronin, Modern Dispenser Cathodes, IEEE Proc. 128 (1981) 19.

[3] G. Haas, R. E. Thomas, C. R. Marrian, Rapid Turn-On of Shelf-Stored Tubes: An Update, IEEE Trans. Elect. Dev. 38 (1991) 2244–2251.

[4] T. Verhey, Microanalysis of Extended-Test Xenon Hollow Cathodes, 27th Joint Propulsion Conference, Sacramento, CA. (1991) AIAA-91-2123.

[5] T. Sarver-Verhey, Destructive Evaluation of a Xenon Hollow Cathode After a 28,000 Hour Life Test, in: 34rd Joint Propulsion Conference, Cleveland, OH. (1998) AIAA-98-3482.

[6] J. Brophy, C. Garner, A 5,000 Hour Xenon Hollow Cathode Life Test, 27th Joint Propulsion Conference, Sacramento, CA. (1991) AIAA-91-2122.

[7] P. Suitch, Thermochemical Reactions in Tungsten-Matrix Dispenser Cathodes Impregnated with Various Barium-Calcium-Aluminates, Ph.D. thesis, Georgia Institute of Technology, Atlanta, GA (1987).

[8] J. Polk, J. Anderson, J. Brophy, V. Rawlin, M. Patterson, J. Sovey, The Results of an 8200 Hour Wear Test of the NSTAR Ion Thruster, in: 35th Joint Propulsion Conference, Los Angeles, CA. (1999) AIAA-99-2446.

[9] A. Sengupta, Destructive Physical Analysis of Hollow Cathodes from the Deep Space 1 Flight Spare Ion Engine 30,000 Hr Life Test, 29th International Electric Propulsion Conference, Princeton, NJ. (2005) IEPC 2005-026.

[10] J. Polk, I. Mikellides, I. Katz, A. Capece, Tungsten and barium transport in the internal plasma of hollow cathodes, J. Appl. Phys., 105 (2009) 113301.

[11] L. Schoenbeck, D. Hill, R. Shafer, W. Ohlinger, Barium Source Material Development for Reservoir Hollow Cathodes, 40th Joint Propulsion Conference, Fort Lauderdale, FL. (2004) AIAA-2004-4209.

[12] J. Polk, The Effct of Reactive Gases on Hollow Cathode Operation, 41st Joint Propulsion Conference, Sacramento, CA. (2006) AIAA-2006-5153.

[13] J. Polk, D.Goebel, R. Watkins, K. Jameson, L. Yoneshige, J. Przybylowski, L. Chu, Characterization of Hollow Cathode Performance and Thermal Behavior, 41st Joint Propulsion Conference, Sacramento, CA. (2006) AIAA-2006-5150.

[14] J. Polk, Long and Short Term Effects of Oxygen Exposure on Hollow Cathode Operation, 43rd AIAA Joint Propulsion Conference, Cincinnati, OH. (2007) AIAA-2007-5191.

[15] J. Polk, C. Marrese-Reading, B. Thornber, L. Dang, L. Johnson, I. Katz, Scanning Optical Pyrometer for Measuring Temperatures in Hollow Cathodes, Rev. Sci. Instrum. 78 (2007) 093101.

[16] T. Sarver-Verhey, Scenario for Hollow Cathode End-of-Life, 26th International Electric Propulsion Conference, Kitakyushu, Japan. (1999) IEPC-99-126.

[17] K. Jameson, D. Goebel, R. Watkins, Hollow Cathode and Keeper-Region Plasma Measurements, 41st Joint Propulsion Conference, Tucson, AZ. (2005) AIAA-2005-3667.